CRYSTALLIZATION BEHAVIOR OF CLAY NANOCOMPOSITES PREPARED FROM A DEGRADABLE ALTERNATING COPOLYESTER CONSTITUTED BY GLYCOLIC ACID AND 6-HYDROXYHEXANOIC ACID

Laura Morales,[1,2] Lourdes Franco,[1,2] María Teresa Casas,[1] Jordi Puiggalí[1,2]

[1]Departament d'Enginyeria Química, Universitat Politècnica de Catalunya, Av. Diagonal 647, E-08028, Barcelona, SPAIN

[2]Centre de Recerca en NanoEnginyeria (CRNE), Universitat Politècnica de Catalunya, Edifici C', c/ Pascual i Vila s/n, E-08028, Barcelona, SPAIN

Introduction

Aliphatic polyesters constitute nowadays the main family of degradable polymers due to the presence of hydrolizable ester groups. However, in general mechanical and thermal properties are not adequate to satisfy the requirements for their use in applications such as packing materials. Properties of materials can also be considerably modified by the incorporation of layered silicates into the polymer matrices. The resulting biodegradable nanocomposites possess several advantages generally attained at low silicate content (less than 5%). Although, biodegradable nanocomposites have very strong future prospects the present low level of production and high costs still restrict them form a wide range of applications.

The aims of this work are to prepare an exfoliated nanocomposite from a new biodegradable copolyester constituted by an alternating distribution of glycolic acid and 6-hydroxyhexanoic acid units, and to study the influence of clay particles on the isothermal crystallization process. Thus, overall crystallization rate, crystal growth rate and change of morphological parameters during crystallization are analyzed for both the pristine and the nanocomposite samples by using different techniques.

Nanocomposite Preparation

An exfoliated nanocomposite was prepared by the film-casting technique from the C25A organo-modified clay and a new biodegradable polyester derived from glycolic acid and 6-hydroxyhexanonoic acid. This polyester has a sequential monomer distribution and high crystallinity, allowing a detailed study of its isothermal crystallization.

$$\mathrm{ClCH_2COCl + HO(CH_2)_5COOH} \xrightarrow{\mathrm{CHCl_3,\ KHCO_3/H_2O}} \mathrm{ClCH_2COO(CH_2)_5COO^-K^+} \xrightarrow{\mathrm{Vacuum},\ \Delta} \mathrm{-[OCH_2COO(CH_2)_5CO]_x- + KCl}$$

Poly(glc-*alt*-6HH)

X-ray diffraction and Transmission Electron Microscopy

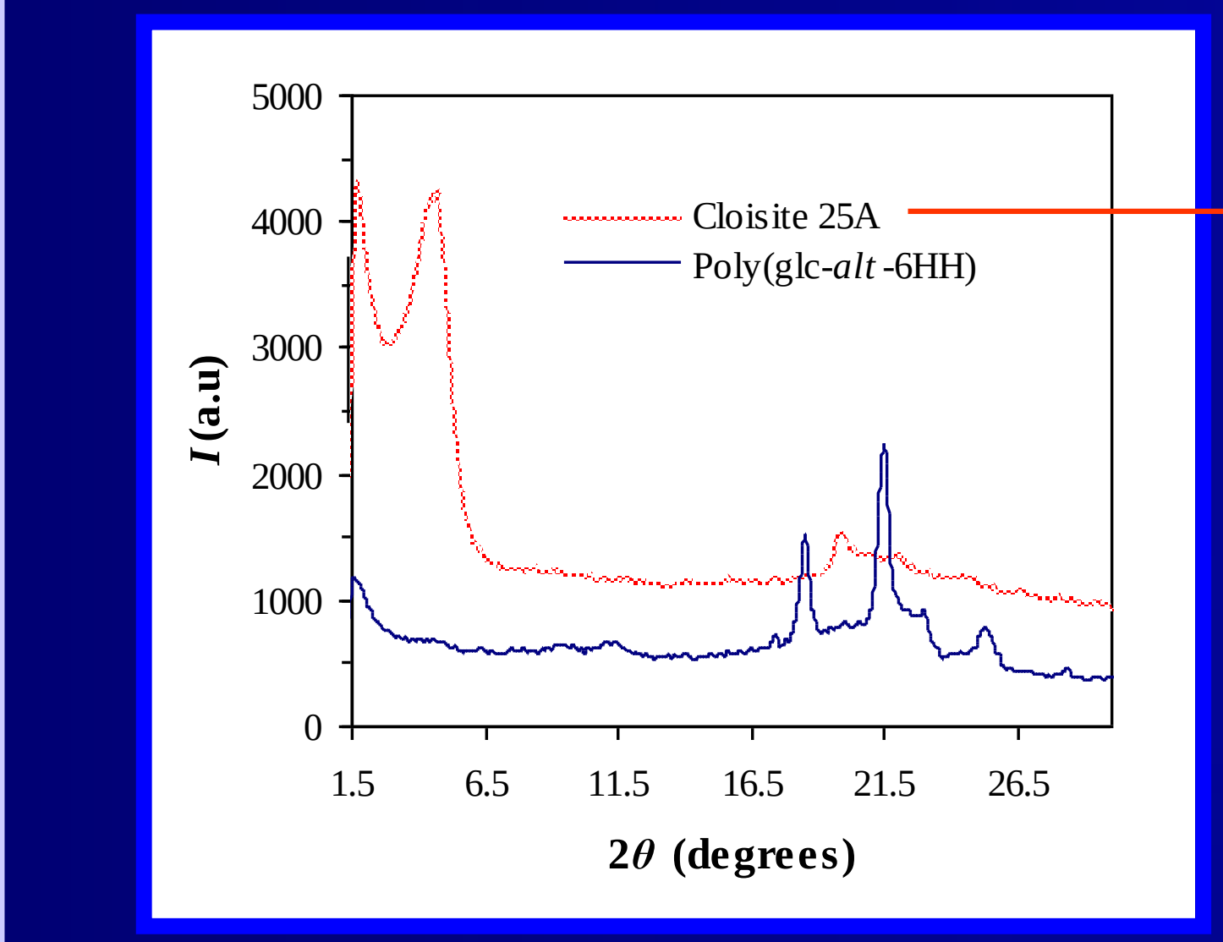

CLOISITE C25A

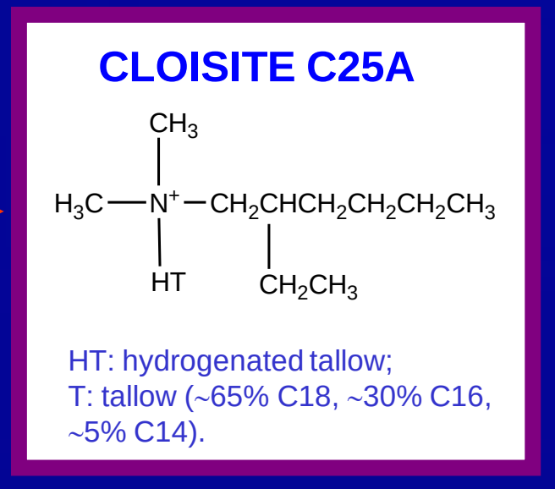

$$\mathrm{H_3C{-}N^+(CH_3)(HT){-}CH_2CH(CH_2CH_3)CH_2CH_2CH_2CH_3}$$

HT: hydrogenated tallow;
T: tallow (~65% C18, ~30% C16, ~5% C14).

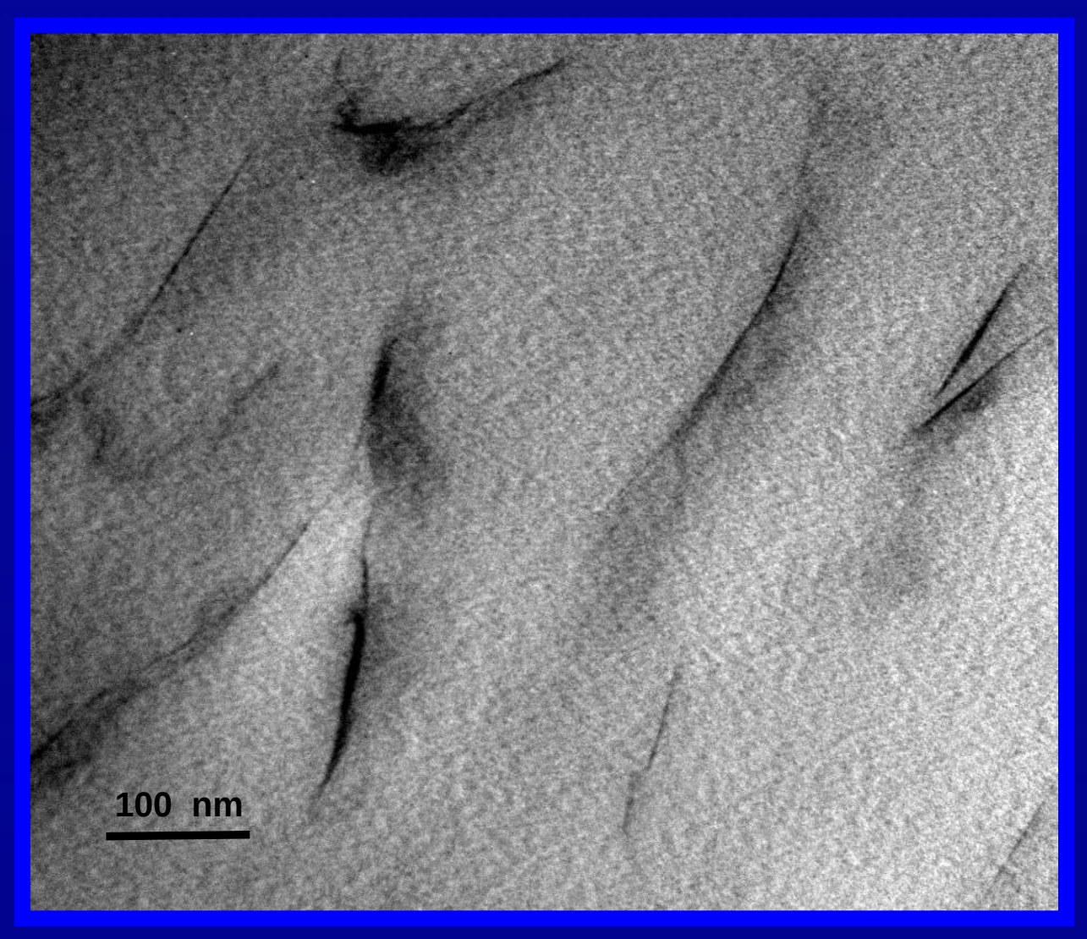

The samples were studied by means of X-ray diffraction and transmission electron microscopy. It was obtained an exfoliated structure by the film-casting technique from the addition of C25A organoclay.

FTIR Analysis

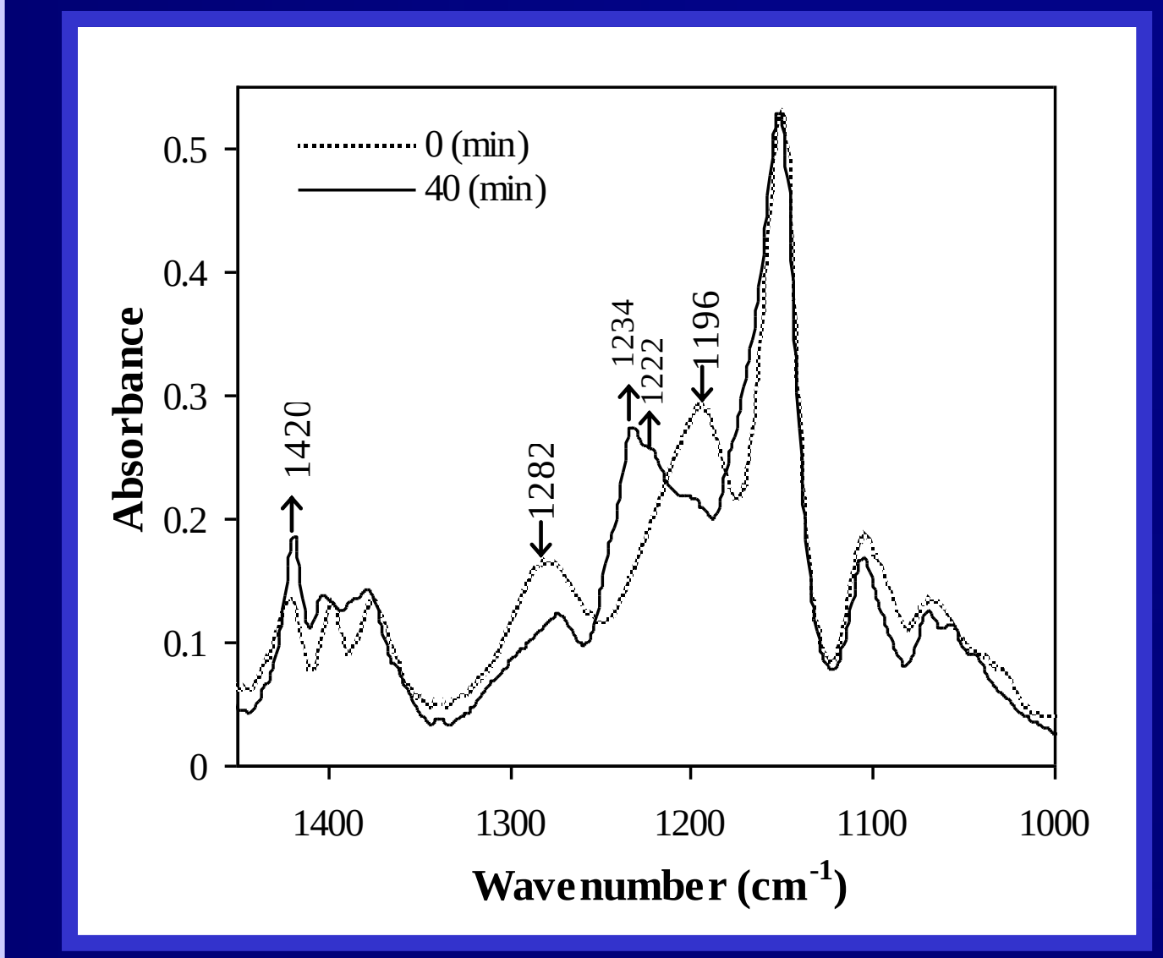

Absorption FTIR spectra (1500-1000 cm^{-1}) of the neat polyester at the beginning and at the end of isothermal crystallization at 50ºC

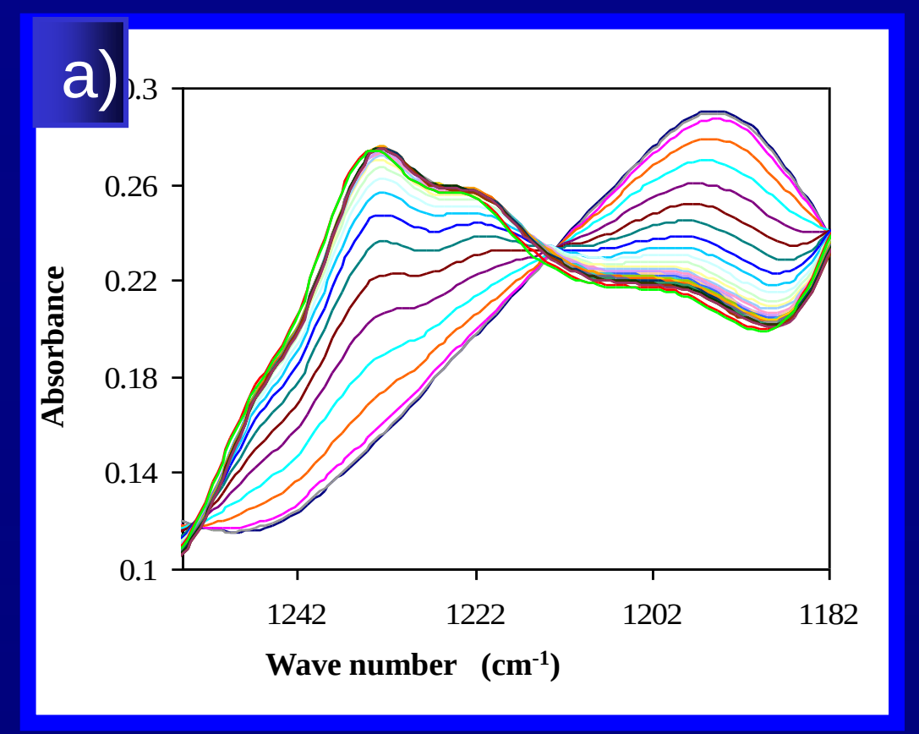

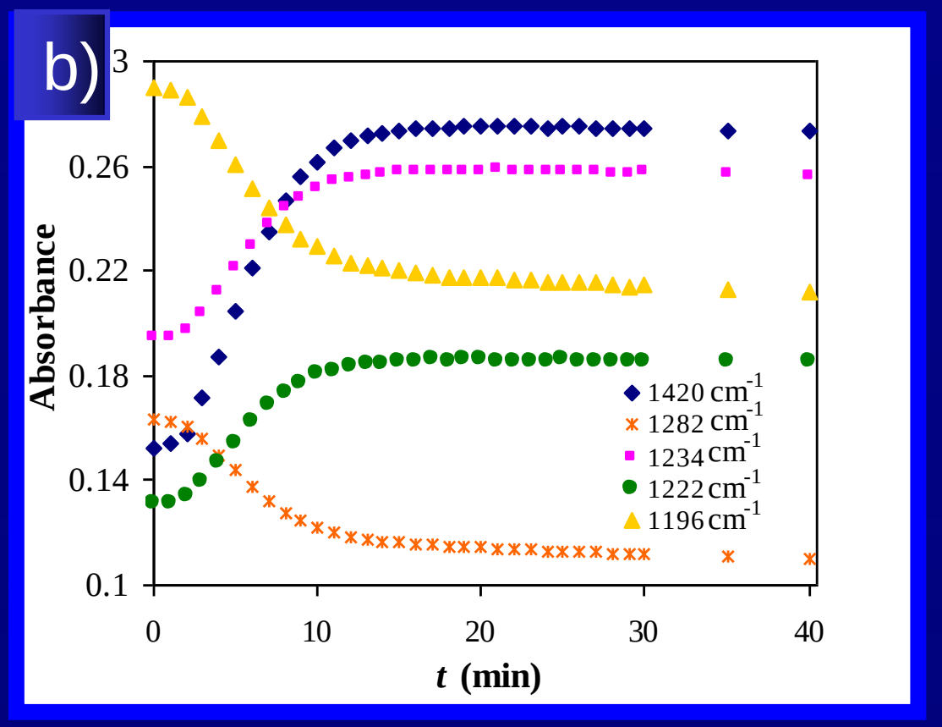

a) Changes in the infrared absorption bands at 1234 and 1222 cm^{-1} of the neat polyester during isothermal crystallization at 50ºC

b) Time evolution of the absorption of selected infrared bands for isothermal crystallization at 50ºC of the neat polyester. Characteristic bands of the amorphous (1282 and 1196 cm^{-1}) and crystalline phases (1420, 1234 and 1222 cm^{-1}) were chosen

FTIR is highly sensitive to molecular conformation and packing density, hence its usefulness in polymer crystallization studies. Characteristic bands can be correlated to the crystalline and amorphous phases of the bulk and typically remain distinguishable over the course of crystallization. Different bands in this region can be assigned to the crystalline (1420, 1234 and 1222 cm^{-1}) or the amorphous phase (1282 and 1196 cm^{-1}) since their absorptions increase or decrease, respectively, during the crystallization process

Optical microscopy studies and Calorimetric Data.

Primary nucleation and crystal growth rate decreased significantly with the incorporation of nanoparticles. The overall crystallization rate of the nanocomposite was lower than that of the neat polyester. A similar equilibrium melting point was derived from both samples.

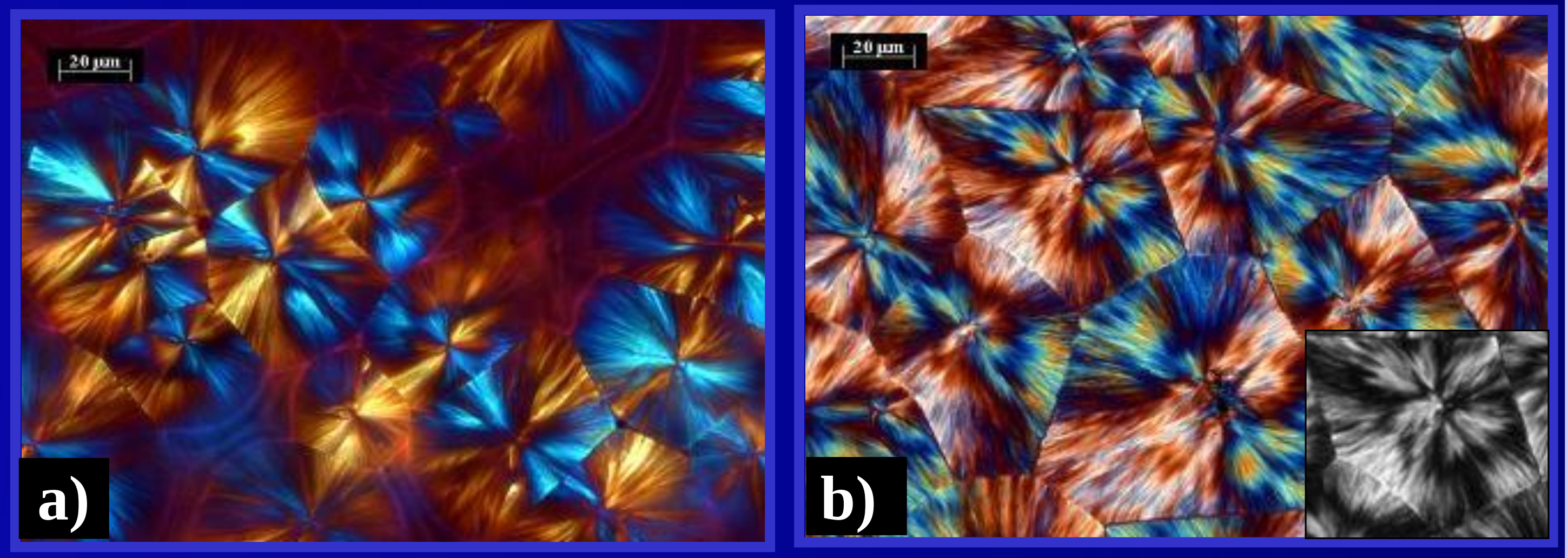

Optical micrographs taken at the end of isothermal crystallization at 54 ºC of the neat polyester (a) and its nanocomposite with 3% of C25A (b). Spherulites of both samples show negative birefringence.

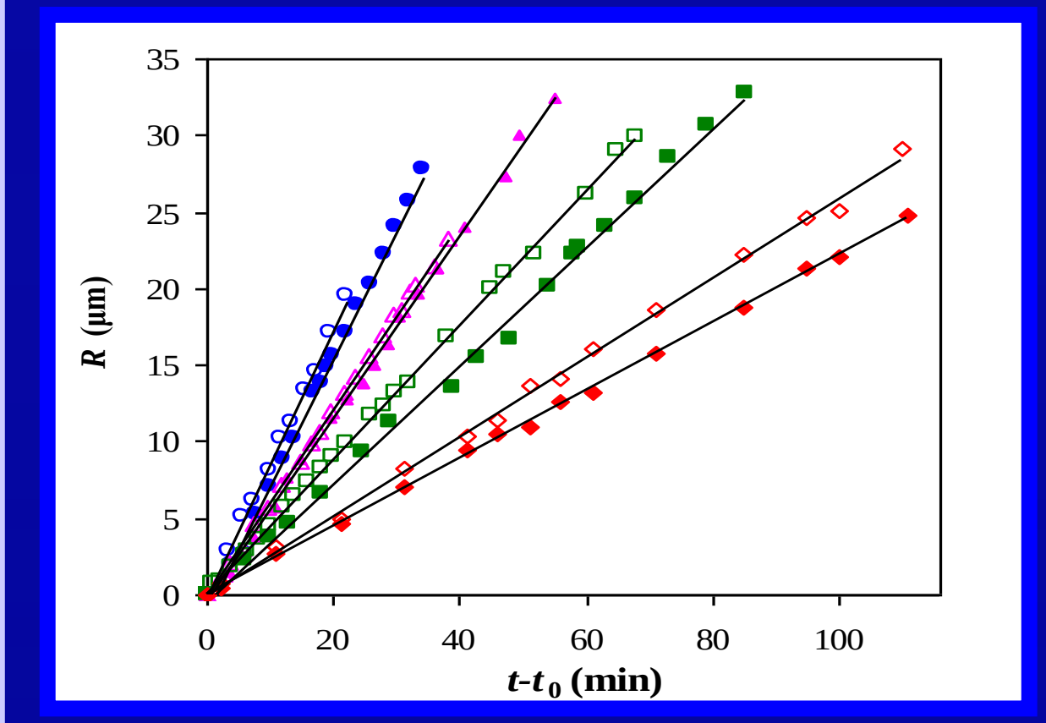

Spherulite radii of the neat polyester (empty symbols) and its nanocomposite with 3% of C25A (full symbols) versus crystallization time.

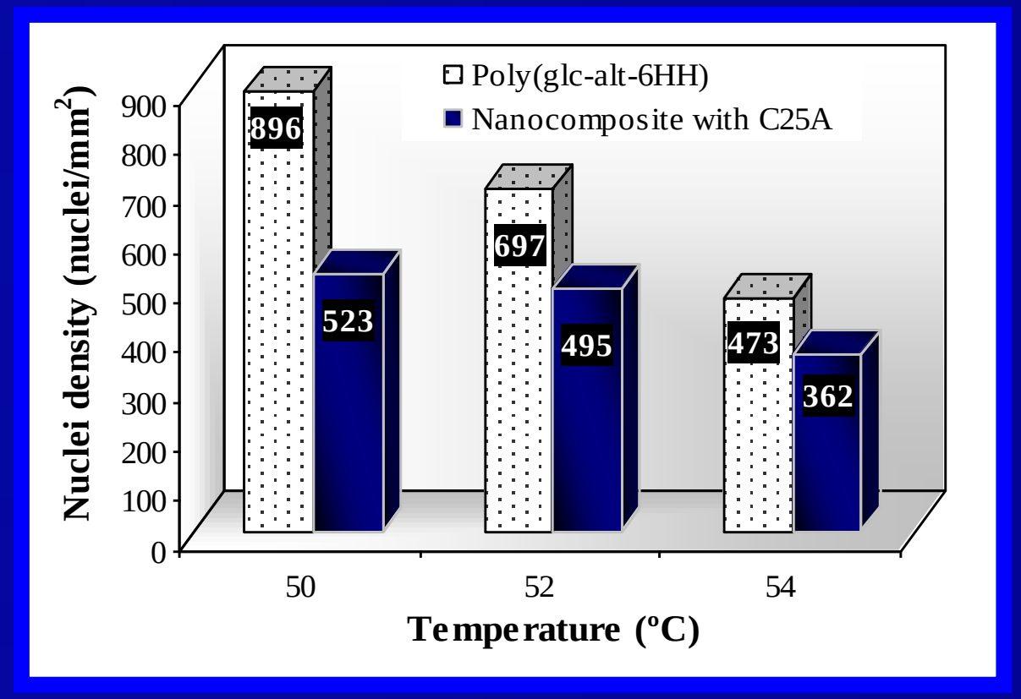

Comparison of the density of nuclei between the neat polyester and its C25A nanocomposite at three crystallization temperatures.

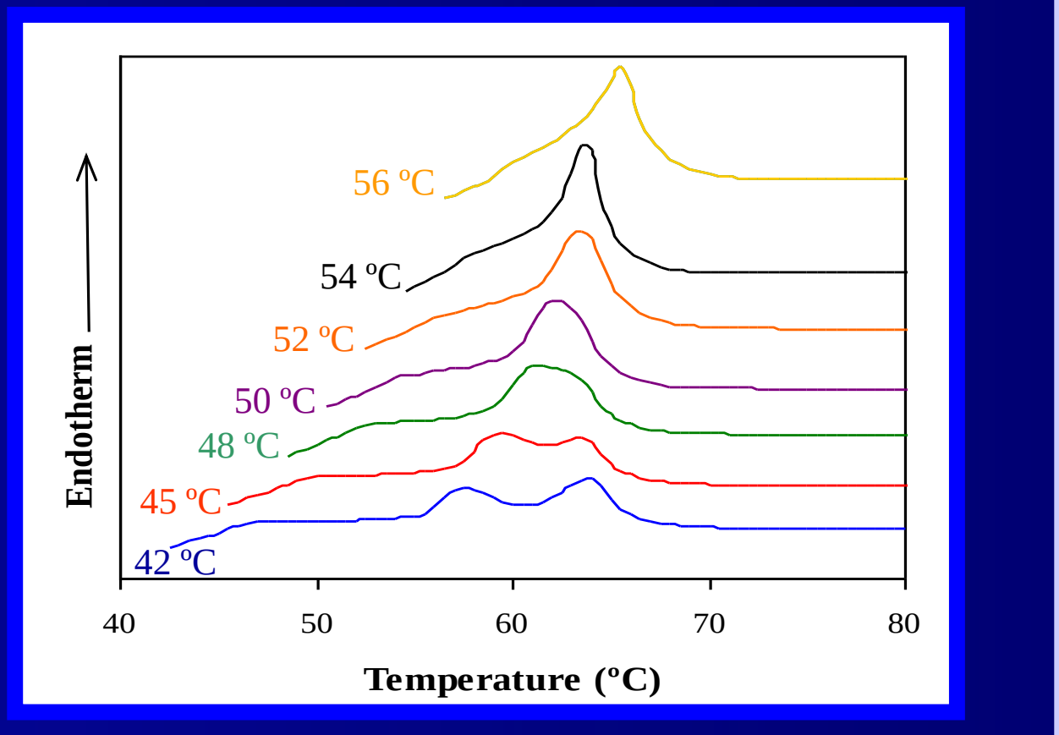

Melting behavior of the poly(glc-*alt*-6HH)/C25A nanocomposite isothermally crystallized at different temperatures.

Crystalline morphology and isothermal crystallization from SAXS/WAXD data

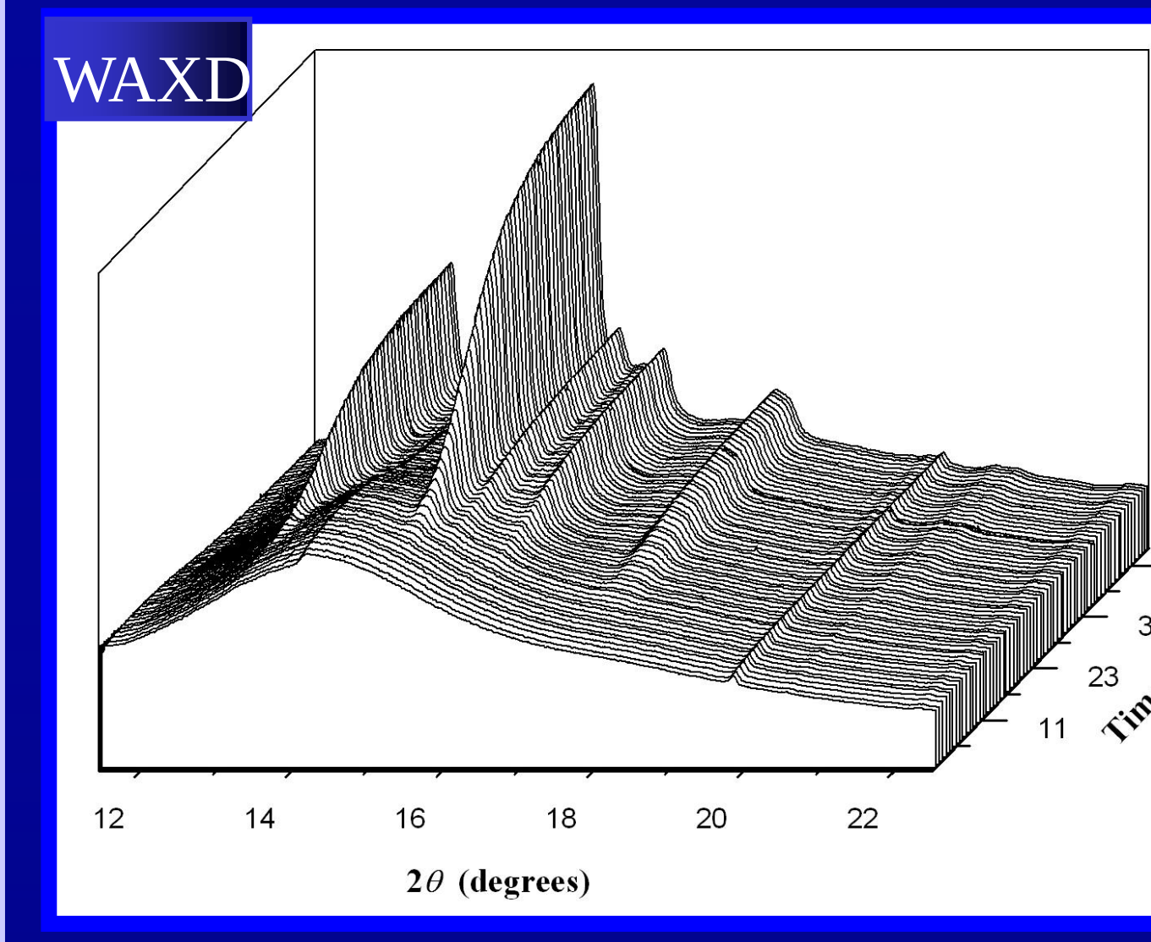

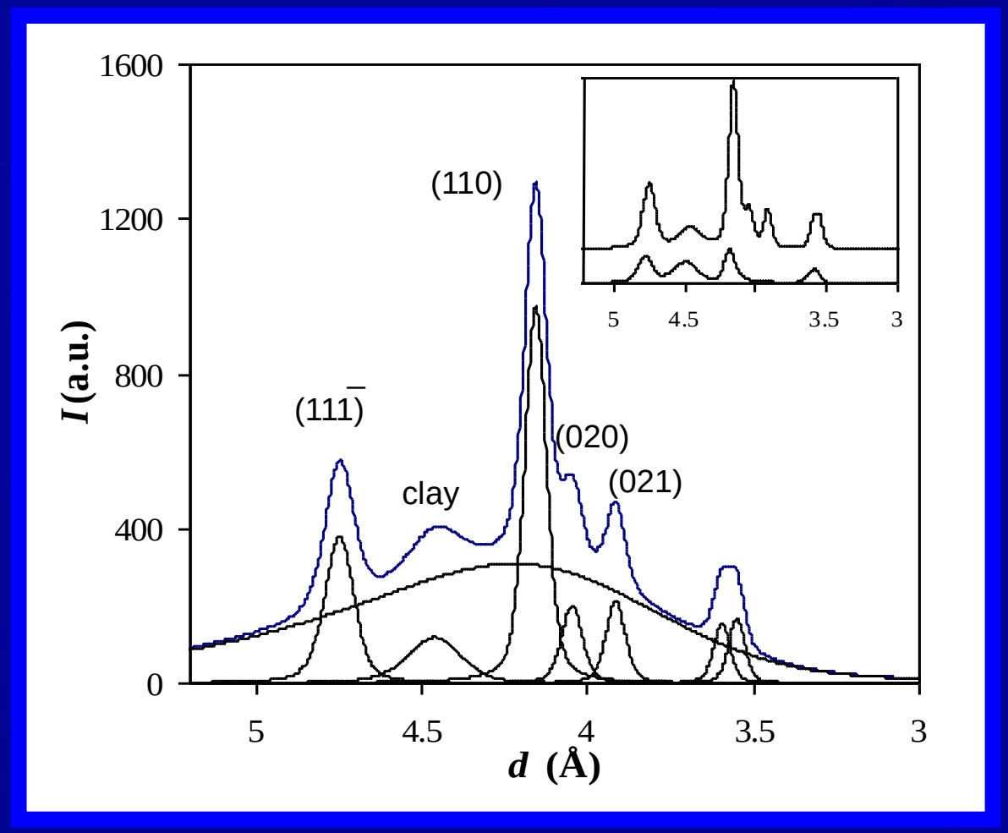

Deconvolution of the WAXD profile of poly(glc-*alt*-6HH)/C25A at 50ºC.

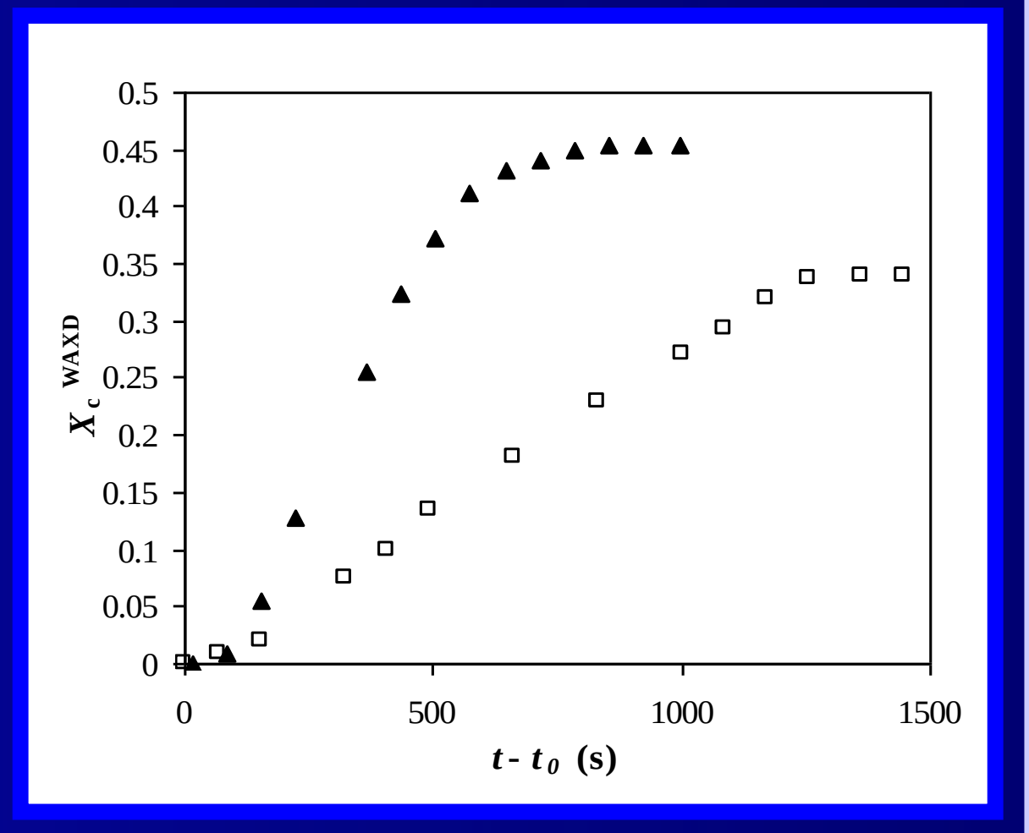

Evolution of crystallinity determined from WAXD at 50ºC of the neat polyester (▲) and its nanocomposite (□).

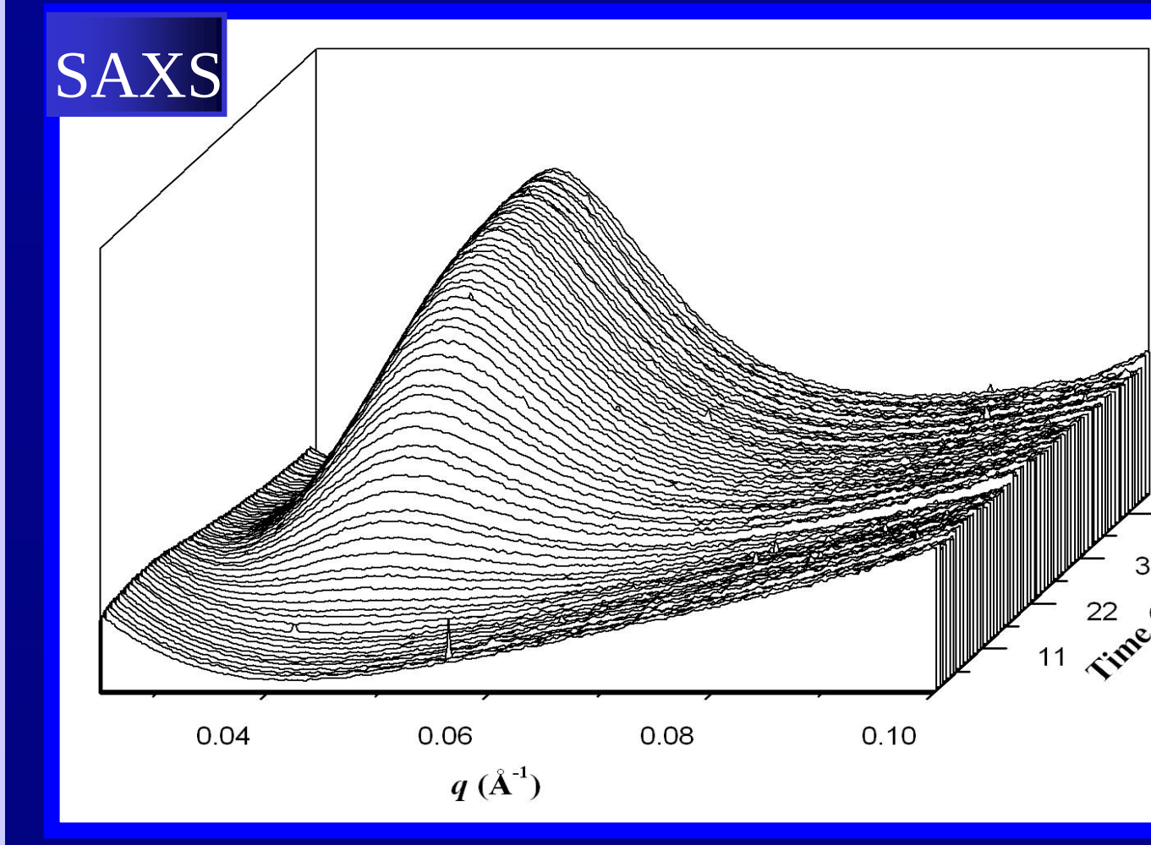

SAXS/WAXD 3-dimensional profiles of poly(glc-*alt*-6HH)/C25A during isothermal crystallization at 54 ºC.

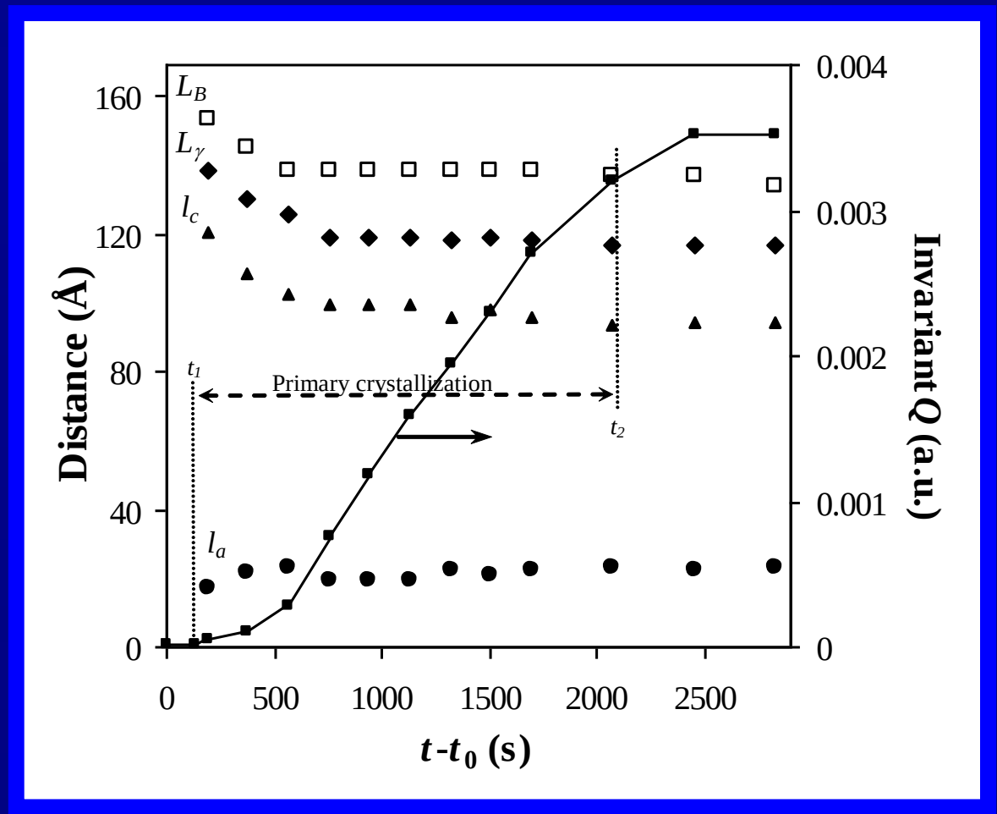

Time evolution of invariant (■), Bragg spacing (□), long period from the correlation function (♦), crystal thickness (▲) and amorphous thickness (●) during isothermal crystallization at 54ºC of poly(glc-*alt*-6HH)/C25A.

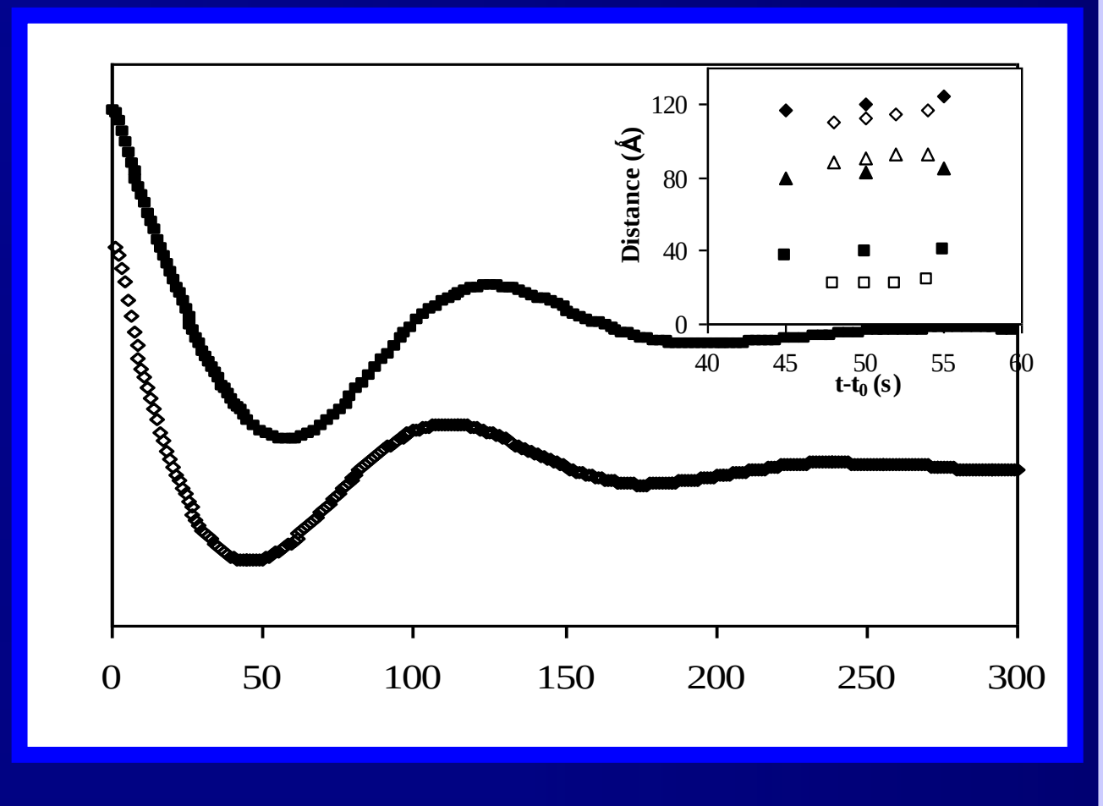

Correlation functions at the end of crystallization at 50 ºC of the neat polyester (■) and its nanocomposite (◊). The inset shows the final L_γ (♦) l_c (▲) and l_a (■) spacings at various crystallization temperatures for the neat polyester (full symbols) and its nanocomposite (empty symbols).

Conclusions

X-ray and TEM observations revealed full dispersion of silicate layers and suggested a high miscibility between the polymer matrix and the clay.

Incorporation of C25A decelerated the mechanism of primary nucleation and crystal growth of poly(glc-alt-6HH), a trend commonly observed when high homogeneous dispersion of silicate layers occurs. A slight increase in the secondary nucleation constant was also inferred for the nanocomposite by considering the Lauritzen and Hoffman treatment.

SAXS data showed significant changes in the morphology of constitutive lamellae since a dramatic decrease in the amorphous layer thickness was observed for the nanocomposite.